frontiers | Frontiers in Membrane Science and Technology

TYPE Original Research
PUBLISHED 21 August 2025
DOI 10.3389/frmst.2025.1653159

OPEN ACCESS

EDITED BY
Soraya Phumzile Malinga,
University of Johannesburg, South Africa

REVIEWED BY
Gyorgy Szekely,
King Abdullah University of Science and Technology, Saudi Arabia
Kok Chung Chong,
Universiti Tunku Abdul Rahman, Malaysia

*CORRESPONDENCE
Farshid Pajoum Shariati,
farshid.pajoumshariati@umontpellier.fr

RECEIVED 24 June 2025
ACCEPTED 30 July 2025
PUBLISHED 21 August 2025

CITATION
Farastoon Dashti SS, Ansari I, Emamshoushtari MM, Helchi S, Lessage G, Heran M and Pajoum Shariati F (2025) Comparison of batch and continuous operation modes for maxilon red azo dye removal using *Chlorella vulgaris* microalgae within photobioreactor (PBR) and a dynamic membrane photobioreactor (DMPBR). *Front. Membr. Sci. Technol.* 4:1653159. doi: 10.3389/frmst.2025.1653159

Comparison of batch and continuous operation modes for maxilon red azo dye removal using *Chlorella vulgaris* microalgae within photobioreactor (PBR) and a dynamic membrane photobioreactor (DMPBR)

Shaghayegh Sadat Farastoon Dashti [1], Iman Ansari [1], Mir Mehrshad Emamshoushtari [1,2], Salar Helchi [1], Geoffroy Lessage [3], Marc Heran [3] and Farshid Pajoum Shariati [1,3]*

[1]Department of Chemical Engineering, Islamic Azad University, Science and Research Branch, Tehran, Iran, [2]Institute of Chemical, Environmental and Bioscience Engineering, TU Wien, Vienna, Austria, [3]Université de Montpellier - Institut Européen des Membranes, Montpellier, France

This study aimed to contrast the effectiveness of Chlorella vulgaris microalgae in decolorizing Maxilon Red, an azo-red dye typically found in textile wastewater. It contrasted the dye removal efficiency of two photobioreactor models, a conventional photobioreactor (PBR) and a dynamic membrane photobioreactor (DMPBR). Batch mode operation was used for the PBR, while the DMPBR was carried out continuously. The initial concentration of dye ranged from 5 to 30 mg L^{-1}. Kinetic analysis was used to check the model that gave the best correlation, and isotherm studies were carried out to explain the adsorption mechanism. Fourier-transform infrared spectroscopy (FTIR) was used to identify functional groups involved in binding with the dye. In the PBR, dye removal efficiency increased from 73% to 86% with a rise in initial dye concentration from 5 to 15 mg L^{-1}, but decreased to 53% at 30 mg L^{-1} due to saturation phenomena. The Elovich model best represented the adsorption kinetics, indicating a heterogeneous surface and decreasing adsorption rate with time. Isotherm data also conformed to the Langmuir model, suggesting monolayer adsorption with a maximum of 8.16 mg g^{-1} capacity. FTIR confirmed the involvement of hydroxyl, carbonyl, and polysaccharide groups in dye binding. DMPBR, operated in continuous mode, achieved greater and constant removal efficiency of approximately 98% at 15 mg L^{-1} due to prolonged and uninterrupted contact between dye and biomass. The continuous DMPBR configuration overcame batch PBR saturation limitations, with enhanced biosorption activity,

process stability, and improved effluent quality. Overall, the DMPBR was more efficient and sustainable in azo dye removal from wastewater than the traditional PBR.

KEYWORDS

dynamic membrane photobioreactor, Chlorella vulgaris, maxilon red, azo dye, wastewater treatment

1 Introduction

The textile industry is known as one of the most water-consuming industries in the world. This heightened water consumption gives rise to the production of extensive volumes of contaminated wastewater, lead to a significant environmental hazard (Siddique et al., 2017). Textile industry wastewater contains pollutants, such as dyes, degradable organic substances, detergents, stabilizing agents, mineral salts, and heavy metals. The textile industry approximately accounts for 17 to 20 percent of water pollution among industries (Jegatheesan et al., 2016). It is estimated that more than 30% of the environmental pollutant chemicals are discharged into the environment by the effluents of various textile and dye processing industries (Desore and Narula, 2018). Azo dyes are considered one of the most problematic dyes in the textile industry. Maxilon Red is one of the most commonly used azo dyes, representing more than 50% of global dye production (Deniz, 2014). Azo dyes are compounds consisting of a diazotized amine coupled to an amine or phenol and contain one or more azo linkages. The essential precursors of azo dyes are aromatic amines. Azo dyes have been shown to have toxic effects, including genotoxicity, mutagenicity, and carcinogenicity in humans and animals. Their indiscriminate disposal, mainly from the textile industry, poses a major threat to public health and the environment (Chung, 2016). Being water-soluble, they increase water turbidity, block light penetration, inhibit photosynthesis, and raise chemical and biological oxygen demand, endangering aquatic life (Bahadur et al., 2020). Additionally, skin contact with dyes can cause allergies and cancer (Sreedharan et al., 2019). Untreated dye-containing wastewater poses serious risks to the biosphere and human health.

Manifold physical and chemical methods have been applied to remove azo dye from wastewater including adsorption (Al-Amrani et al., 2022), ion exchange (Swain et al., 2023), membrane filtration (Jankowska et al., 2022), coagulation/flocculation process (El Gaayda et al., 2024), advanced oxidation (Corona-Bautista et al., 2021), and electrochemical approaches (Hamous et al., 2021). The major limitations of the physical approaches for the treatment of textile dye wastewater are the high cost of operation and maintenance, chemical consumption, inefficiency in removing pollutants at very low concentrations, process complexity, and high energy demand (Kanwal et al., 2022; Kishor et al., 2021). On the other hand, in biological dye removal methods from wastewater, microorganisms such as bacteria, microalgae, and fungi contribute to biodegradation, decomposition, and uptake of dye from the wastewater (Al-Tohamy et al., 2022). Biological methods are considered eco-friendly, cost-effective, energy saving, and fewer chemical reagents required (Kishor et al., 2021). Microalgae have a high potential to remove dye from textile wastewater. During this process, the dyes in textile wastewater are removed through biotransformation and biodegradation, and invaluable microalgal biomass is produced (Chan et al., 2014). The biosorption capability of microalgae can be related to the high surface area and high binding affinity during the treatment process. Furthermore, the microalgae cell surface has a wide range of functional groups such as hydroxyl carboxylate and amino phosphate that are responsible for the accumulation dye on the surface of the microalgae cell biopolymer (Hernández-Zamora et al., 2015; Zheng et al., 2020). Microalgae such as *Chlorella vulgaris*, *Daphnia magna,* and *Ceriodaphnia dubia* can absorb Congo Red (CR) dye depending on their molecular structure. *Chlorella vulgaris* has been shown to remove 83% and 58% of dye at concentrations of 5 and 25 mg. L^{-1}, respectively, in batch mode (Hernández-Zamora et al., 2015). Moreover, the biomass generated is well-suited for downstream, further aligning with circular economy and sustainability goals (Barani et al., 2025). This is because valuable microalgal biomass is generated throughout the wastewater treatment process, which is characterized by a high concentration of proteins, amino acids, vitamins, minerals, antioxidant substances, and other bioactive compounds (Nasser et al., 2023), that can be utilized in the several sectors including medicine, biodiesel, bioplastics, biofertilizers, single-cell proteins, aqua culturing, treating greenhouse gases, and wastewater treatment (Barani et al., 2025; Gupta et al., 2015; Helchi et al., 2023). Microalgal by-products from wastewater can be safe for human or animal consumption if strict controls ensure the removal of heavy metals, organic pollutants, and pathogens. Studies show that proper cultivation and decontamination, including selecting non-toxic strains and using closed reactors, can allow biomass to meet EU safety thresholds (Park et al., 2024). Although species-specific accumulation (like that of Cd and Hg) necessitates regular ICP-MS and HPLC monitoring to ensure levels remain below regulatory limits, microalgae can efficiently bioaccumulate nutrients and adsorb heavy metals while reducing N and P concentrations (Faruque et al., 2024; Sarma et al., 2024). Pathogen risks, such as bacteria, viruses, and protozoa, are decreased by microfiltration and photobioreactor design; data show that Risk Group 2 (RG2) bacteria in pig farm effluents have decreased by over 60% (Álvarez-González et al., 2023; López-Sánchez et al., 2022). By following these steps, wastewater-grown microalgae can be used as a source of bioactives like astaxanthin and ω-3s and as a sustainable, nutrient-rich feed supplement (40%–70% protein) without posing a risk to human or animal health (Saadaoui et al., 2021; Zhang and Lu, 2024). Among microalgae species, *C. vulgaris* has demonstrated its effectiveness in dye biosorption, particularly for cationic and azo dyes (Moradi et al., 2024). Its cell wall structure is rich in functional groups such as hydroxyl, carboxyl, phosphate, and amino, facilitating strong electrostatic and hydrogen bonding interactions with dye molecules (Yadav et al., 2022). *Chlorella vulgaris* is known for its high tolerance to environmental stressors, ease of cultivation, and

rapid biomass growth, even in nutrient-variable conditions such as wastewater (Ezhumalai and Rajkumar, 2025). Prior studies have reported removal efficiencies exceeding 80% for dyes like Congo Red and Methylene Blue using *C. vulgaris* in batch systems. These combined features make *C. vulgaris* a suitable and scalable candidate for integrated wastewater treatment systems (Hernández-Zamora et al., 2015; Lim et al., 2010).

Understanding the adsorption kinetics and isotherms is essential for optimizing the performance of adsorption for dye removal in the batch systems. Kinetic models such as intra-particle diffusion, pseudo-first order, pseudo-second order, and Elovich kinetic models, shed light on how the biosorption process reaches equilibrium. A lot of beneficial information would be extracted from isotherms and adsorption kinetics (Pradhan et al., 2019). In the context of dye-contaminated wastewater, equilibrium isotherm models provide further insights into the interaction between dye molecules and microalgal biomass. The Langmuir isotherm, which assumes monolayer adsorption on a homogenous surface, is commonly used to determine the maximum adsorption capacity and has been successfully applied in studies involving *C. vulgaris* and azo dyes (Hernández-Zamora et al., 2015). The multilayer model, known as the Freundlich model, is classified as a type of interaction between the surface of biomass and adsorbate (Pradhan et al., 2019).

Many studies have been made regarding the effectiveness of microalgae, especially *C. vulgaris*, in removing dyes from textile wastewater, and a massive portion of these investigations have focused on batch systems (Lim et al., 2010; Fazal et al., 2021; Rehman et al., 2024). Considering the utilization of microalgae in wastewater treatment, the objective is to enhance the removal efficiency of pollutants by implementing a continuous treatment process while concurrently producing biomass. In this regard, integrating conventional microalgae cultivation with membrane technology within the membrane photobioreactor (MPBR) is advantageous. Membrane provides higher biodegradation efficiency by increasing the solids retention time (SRT), which would give more time to break down organic pollutants, better-treated water quality, superior control of solids and hydraulic retention time (Emamshoushtari et al., 2022). MPBRs also significantly reduce the required operation area by combining the biodegradation and separation units in one system (Keyvan Hosseini et al., 2023). The mentioned system has also proven beneficial for microalgae harvesting as it enables full biomass retention and is economical (Liao et al., 2018). Nevertheless, it is a significant setback for membrane separation; the deposition of an algal cake layer on the surface of the membrane, known as membrane fouling, may increase energy use due to decreased flow and hydraulic resistance (Vaezi et al., 2025). However, membrane efficiency can be solved by designing a secondary dynamic membrane (DM) on the static membrane for better separation (Emamshoushtari et al., 2022). In one study the authors have evaluated an anaerobic dynamic membrane bioreactor (AnDMBR) for textile wastewater treatment, achieving high removal rates of soluble COD (98.5%) and color (>97.5%). The dynamic membrane effectively rejected large particles, while microbial analysis showed stable archaeal communities and adaptive shifts in bacterial populations, supporting robust anaerobic degradation of dye-laden wastewater (Berkessa et al., 2020). In another study the authors have evaluated a living membrane bioreactor (LMBR) using an encapsulated self-forming dynamic membrane (ESFDM) for treating synthetic textile wastewater. The system achieved high removal efficiencies for COD (96%), dyes (~85–86%), ammonia (97%), and moderate sulfate removal (~41%), while effectively limiting membrane fouling. The treated effluent met regulatory discharge standards, highlighting the LMBR's potential as a cost-effective and scalable solution for textile wastewater treatment (Jallouli et al., 2023). It should be noted that all these studies were done using activated sludge systems. The additional capability of removing heavy metals, shown by the microalgae through this wastewater treatment process, contributes to the broadened efficiency and profitability of the overall process. DM is also easily separable from the membrane when washing or with a reverse airflow/water stream, and also it facilitates microalgae cultivation from the system (Emamshoushtari et al., 2022; Fard and Mehrnia, 2017), and facilitates microalgae harvesting without a subsequent separation operation despite PBR (Fazal et al., 2021). Table 1 shows a comprehensive review regarding the utilization of *C. vulgaris* microalgae in removing pollutants from wastewater.

This study aims to investigate the adsorption isotherms and kinetics of Maxilon Red dye removal using *Chlorella vulgaris* microalgae within a conventional batch PBR. After finding the optimum dye concentration, yielding the highest amount of dye removal, the optimum concentration would again be put into operation. Furthermore, the study will use a dynamic membrane photobioreactor (DMPBR), which operates as a continuous system, to compare the efficiency of batch PBR and DMPBR. This integration not only overcomes the limitations of batch systems but also boosts biomass production, improves dye removal efficiency, and supports more stable, scalable, and energy-efficient wastewater treatment processes. Recognizing that continuous systems are often preferred in industrial applications due to time efficiency, the study develops a DMPBR setup that unites biological nutrient degradation and physical separation in a single continuous process, comparing its performance with that of the conventional batch-operated PBR to determine the operational and environmental advantages in textile wastewater treatment.

2 Materials and methods

2.1 DMPBR setup

Both batch PBR and continuous DMPBR system were made of plexiglass with dimensions of 32 cm in height, 32 cm in length, and 30 cm in width, and a working volume of 24 L. It is illustrated schematically in Figure 1. A sparger connected to an air pump with an aeration rate of 20 L min^{-1} is installed at the bottom of the batch PBR and DMPBR. In this study, a Kubota flat sheet membrane (Osaka, Japan) was immersed in the DMBPR. Table 2 presents the characteristics of the membrane.

The DMPBR operated continuously at room temperature during which synthetic wastewater was treated through the dynamic membrane. The membrane had a filtration area of 0.11 m^2, and the system was operated at a flux of 18 L m^{-2}. h^{-1}, resulting in a permeate flow rate of 1.98 L h^{-1}. The hydraulic retention time (HRT) was approximately 12 h.

TABLE 1 A comprehensive review of similar studies done for the utilization of *Chlorella vulgaris* microalgae for wastewater treatment.

Reactor type	Biological agent	Contaminant	Key findings	References
Batch photobioreactor	*Chlorella vulgaris*	Textile dyes (e.g., Methylene Blue)	~70–90% dye removal in batch mode	Lim et al. (2010)
Batch system	*Chlorella vulgaris*	Congo red	Up to 83% removal efficiency	Hernández-Zamora et al. (2015)
Open raceway	*Chlorella vulgaris*	Nitrate Phosphate	Nearly 100% removal for both pollutants	Wang et al. (2021)
Erlenmeyer flasks	*Chlorella vulgaris*	Nitrate Phosphate Chemical oxygen demand (COD) Biological oxygen demand (BOD)	~70% Nitrate ~100% Phosphate ~13% COD; and ~31% BOD removal	Madadi et al. (2021)
Dynamic membrane photobioreactor (DMPBR)	*Chlorella vulgaris*	Nickel (metal ion)	72% removal efficiency; good membrane stability	Emamshoushtari et al. (2022)

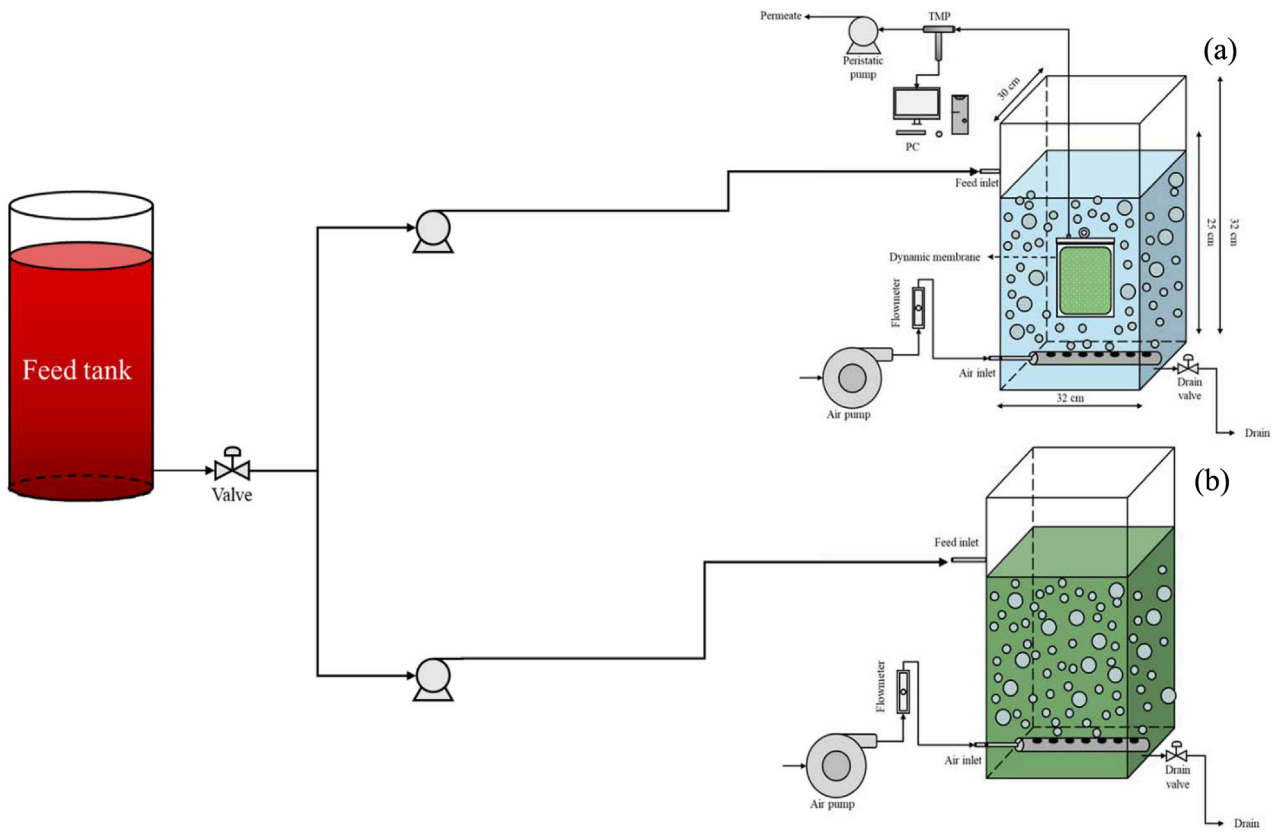

FIGURE 1
The schematics of DMPBR **(a)**, and conventional batch PBR **(b)**.

2.2 Microalgae strains and culture conditions

The microalgae used in this experiment was *Chlorella vulgaris*, a kind of round-shaped green algae well known for its dye-removal capability from dye-contaminated wastewater (Chin et al., 2020). The microalgae bank of the Science and Research Branch of Islamic Azad University in Tehran, Iran, provided *C. vulgaris*. The culture medium used for its growth was based on BG-11 (Emamshoushtari et al., 2022).

The *C. vulgaris* inoculation into 30-L batch PBR, and DMPBR was 5% v. v^{-1} with a dry weight (DW) of about 0.5 g. L^{-1}. The microalgae were exposed to a light-dark regime 24:0 under white LED lamps with an intensity of 3000 lux. When DW reached 2.5 g. L^{-1}

TABLE 2 The characteristics of the membrane.

Type of module	Flat sheet, kubota (H 203), Japan
Pore size	0.4 μm
Filtration area	0.11 m^2
Number of flat sheets	1
Filter plate	ABS
pH	1–10
Membrane material Operating pressure	Polyethersulfone (PES) 0.03–0.4 bar

in both batch PBR and DMPBR systems, the experiments regarding the Maxilon red dye removal were initiated.

DM was formed on the surface of the membrane in the DMPBR. As the microalgae-dynamic membrane forms, the transmembrane pressure (TMP) steadily increases; this would indicate the formation of microalgae as a cake layer on the membrane's surface. It was determined that if the TMP reaches a threshold of 200 bar, the formation of microalgae DM was assumed to be complete.

2.3 Synthetic wastewater preparation

Maxilon Red dye, also known as Astrazon Red FBL; C.I. Basic Red 46; Cationic Red GRL, its chemical structure is 1,2-dimethyl-3-((4-(methyl (phenylmethyl)amino)phenyl)azo)-1,2,4 thiazolium bromide (Farouq, 2022). The dye concentration range in textile wastewater was selected between 10 and 50 mg L^{-1} based on values reported in the literature (Yaseen and Scholz, 2019).

2.4 Scanning electron microscope (SEM)

A microscopic analysis was conducted on the morphology of *C. vulgaris* before and after the removal of dye. Microscopic images were captured using an acceleration voltage of 25 kV and magnifications of 500. These images were then analyzed using a SEM.

2.5 FTIR analysis

Fourier-transform infrared (FTIR) was adopted to determine the functional groups that contributed to the adsorption of Maxilon Red dye by *C. vulgaris*, using a Thermo Scientific Nicolet NEXUS 870 FT-IR spectrometer (United States). The samples of microalgal biomass were collected before and after dye adsorption, washed with deionized water to clear off any residual dye or culture medium, freeze-dried, and ground into powder. An amount equal to 1 mg of the sample was mixed in with 100 mg of spectroscopic-grade potassium bromide (KBr) pressed onto a clear pellet in a hydraulic press. FTIR spectra spanning a 400–4000 cm^{-1} range were recorded at a resolution of 4 cm^{-1}, averaging 32 scans per sample.

2.6 Analytical methods

The dye removal efficiency was determined according to the literature (da Rosa et al., 2018). Briefly, a sample is taken from the system and filtered using filter paper to separate microalgae from the solution. Hence, cotton filters Whatman 1442–125, whose pore size is 2.5 µm, have been used. A spectrophotometer (Hack DR6000 UV VIS) was used to measure the optical absorption of the filtered sample at a 554 nm wavelength. The dye removal efficiency was obtained according to Equation 1:

$$R = \frac{C_0 - C_i}{C_i} \times 100 \quad (1)$$

where R is the color removal efficiency (%), and C_0 and C_i are the initial color concentration and the color concentration after filtration (mg. L^{-1}), respectively.

Moreover, microalgae DW was measured according to the literature (Shirazi et al., 2024). 50 mL of each sample were centrifuged at 10,000 g and 5°C for 20 min to separate the culture medium from the biomass. It was dried at 80°C for 24 h and then weighed.

2.7 Kinetic study

The mechanism of biosorption can be clarified through kinetic studies. Once the kinetic parameters are determined, they provide essential information for reactor design, particularly concerning reactor volume and residence time. Therefore, identifying the kinetic model that best describes the system is critically important.

The equilibrium adsorption capacity of Cr (III) for each sample was calculated using the following equation:

$$q_e = \frac{(C_0 - C_e)V}{m} \quad (2)$$

where q_e shows the biosorption capacity at equilibrium (mg.g^{-1}), V is the volume of the solution (L), C_0 is the initial concentration of the dye (mg.L^{-1}), C_e stands for the equilibrium concentration of the dye (mg.L^{-1}), and m is the mass of the adsorbent (g).

The biosorption capacity of Cr (III) at various time intervals was quantified using Equation 3.

$$q_t = \frac{(C_0 - C_t)V}{m} \quad (3)$$

where, q_t is the biosorption capacity (mg. g^{-1}), and C_t is the concentration of dye in each time step interval.

2.7.1 Pseudo-first order kinetic

Equation 4 provides the pseudo-first-order kinetic equation in differential form (Maleki et al.).

$$-ln(q_e - q_t) = k_1 t - ln(q_e) \quad (4)$$

where k_1 (min^{-1}) represents the pseudo-first-order rate constant. It is possible to determine the values of k_1 and $-ln(q_e)$ by calculating the slope and intercept of a graph plotted between $-ln(q_t - q_e)$ and t.

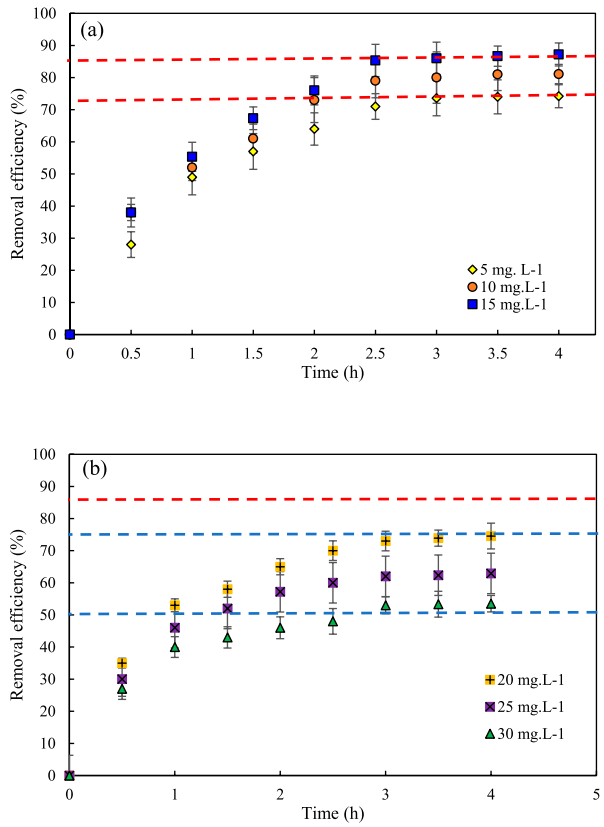

FIGURE 2
Removal efficiency of Maxilon Red dye by *Chlorella vulgaris* *versus* time at different initial dye concentrations, **(a)** 5, 10, and 15 mg. L^{-1}; **(b)** 20, 25, and 30 mg. L^{-1}. Red and blue dashed lines indicate efficiency benchmarks. Error bars represent standard deviations (n = 3).

2.7.2 Pseudo-second-order kinetic

The differential version of the pseudo-second-order kinetic equation is presented in Equation 5 (Sarma et al., 2024).

$$\frac{1}{q_e - q_t} = k_2 t + \frac{1}{q_e} \tag{5}$$

where the pseudo-second order rate constant is indicated by k_2 (in g.mg^{-1}. min^{-1}), a graph of $1/(q_e - q_t)$ *versus* t was created using the experimental data, and the slope and intercept were identified to be k_2 and $1/q_e$, respectively.

2.7.3 Elovich model

The Elovich equation is a valuable model for the qualitative analysis of chemisorption processes. The linearized form of the Elovich model is presented in Equation 6.

$$q_t = \frac{1}{\beta}\ln(\alpha\beta) + \frac{1}{\beta}\ln(t) \tag{6}$$

The biosorption rate (mg.g^{-1}. min^{-1}) and the chemisorption activation energy (g.mg^{-1}) are represented by α and β, respectively, in this equation. Additionally, a graph of q_t vs. l $n(t)$ was produced to determine its slope and intercept, yielding the values of $1/\beta$ and $1/\beta\, ln\, (\alpha\beta)$, respectively.

2.7.4 Intra-particle diffusion model

According to the intra-particle diffusion model proposed by Weber and Morris (Pradhan et al., 2019), the initial rate of intra-particle diffusion is calculated through the linearization of the curve $q = f(t^{0.5})$ (Equation 7):

$$q_t = k_{id} \times t^{0.5} + C \tag{7}$$

where, k_{id} is the coefficient of intra-particle diffusion and C is related to boundary layer.

The graph of (q_t) plotted *versus* $(t^{0.5})$ should construct a straight line.

2.8 Data analysis

The statistical analysis of the results was conducted using analysis of variance (ANOVA). Differences between means were considered significant when the p-value was less than or equal to 0.05. All the experiments were repeated three times at room temperature (25°C ± 2°C).

3 Result and discussion

3.1 Dye removal performance

3.1.1 Dye removal performance via batch PBR containing microalage

As illustrated in Figures 2a,b, the removal efficiency of Maxilon Red dye is observed in the supernatant with the dye's initial concentrations ranging from 5 to 30 mg. L^{-1}.

As indicated in Figure 2, the removal efficiency in supernatants initially increases within the first 3 hours of overall dye concentrations, indicating a fast uptake of dye by *Chlorella vulgaris*. This initial removal phase can be attributed to the high availability of active binding sites on the microalgae surface, which would be further discussed in the FTIR analysis section. It is a fact that suspended microalgae cells have enhanced mass transfer rates between phases due to complete mixing (Emamshoushtari et al., 2022). In this condition, microalgae cells are in constant motion within the photobioreactor, moving and migrating extensively and coming into contact with pollutants at a high rate (Rüdisüli et al., 2012). The dye removal changes in the supernatant were negligible beyond 3 hours, indicating that the adsorption had reached equilibrium (Acuner and Dilek, 2004).

The removal percentage of Maxilon red after 3 hours of contact time in the PBR increased from 73% to 86% when the initial dye concentration increased from 5 mg. L^{-1}–15 mg. L^{-1}. Increasing initial dye concentration increases the likelihood of contact between dye molecules and the biosorbent (Gupta and Suhas, 2009).

In contrast, the removal percentage decreased from nearly 75% to almost 53% when the initial concentration increased from 20 mg. L^{-1}–30 mg. L^{-1}. This may be explained by the fact that the available binding sites are getting filled by microalgae cells, leading to a decrease in removal efficiency (Yagub et al., 2014).

Similar results has been reported in the literature (Özcan et al., 2005; Yagub et al., 2012; Zhang et al., 2012). For example, Yagub

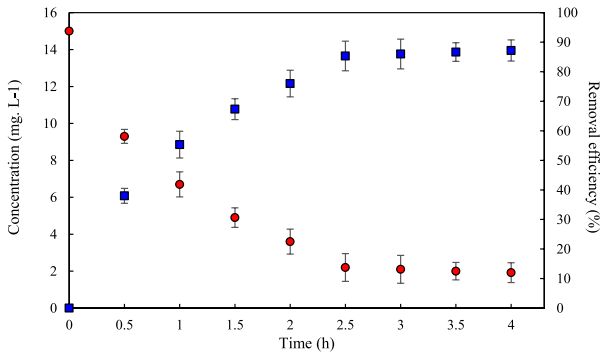

FIGURE 3
Effect of contact time on the Maxilon red removal efficiency at DW = 2.5 g. L^{-1} of micro algae and with initial dye concentration of 15 mg. L^{-1}.

et al. (2012) examined the impact of initial dye concentrations on pine leaves' adsorption of methylene blue. Their findings indicated that with an increase in the initial dye concentration from 10 to 90 mg L^{-1}, there was a corresponding decline in the percentage of dye removal from approximately 96% to almost 41%. As the initial dye concentration rises, less dye is removed because the adsorption sites on the pine tree leaves get saturated more quickly, leaving fewer sites for subsequent dye molecules. Although higher initial dye concentrations provide a stronger driving force for mass transfer, the removal efficiency decreases as the adsorption sites are occupied. Additionally, as dye concentration increases, more dye molecules compete for the same adsorption sites, reducing the overall effectiveness of removal. Even as the adsorption capacity and the quantity of dye absorbed per Gram of adsorbent increases, the percentage removal decreases due to the adsorbent's limited capacity (Yagub et al., 2012).

Furthermore, desorption becomes more probable at higher concentrations, as the concentration gradient causes adsorbed dye molecules to be released back into the solution, leading to a further decrease in removal efficiency. This phenomenon occurs because the dye concentration in the bulk solution is considerably higher, and the dye molecules on the microalgae surface may be "pushed" back into the solution as the system attempts to reach equilibrium (Rafatullah et al., 2019).

3.2 Adsorption kinetic study

3.2.1 Contact time

Identifying the appropriate kinetic model is crucial to analyzing the time-based variation in dye concentration. Figure 3 shows the relationship between dye concentration and biosorption efficiency as a function of contact time, using an initial dye concentration of 15 mg. L^{-1}.

The biosorption rate was quick at first, reaching an efficiency of 85% within 2.5 h; after that point, no significant change in dye concentration was observed. Consequently, the dye concentration at t = 2.5 h, measured at 2.2 mg. L^{-1}, was considered the equilibrium concentration (C_e). The equilibrium biosorption capacity (q_e) was calculated to be 5.12 mg g^{-1} using Equation 2.

TABLE 3 Kinetic coefficients data for Maxilon red biosorption onto the *Chlorella vulgaris* biomass.

Kinetic models	Coefficients	Value
	q_e experimental	5.12 mg g^{-1}
Pseudo-first-order kinetic	k_1 q_e R^2	1.078 min^{-1} 5.11 mg g^{-1} 0.996
Pseudo-second-order kinetic	k_2 q_e R^2	0.751 g $mg^{-1}.min^{-1}$ 83.33 mg g^{-1} 0.877
Elovich	α β q_e R^2	12.86 mg $g^{-1}.min^{-1}$ 0.61 g mg^{-1} 4.51 mg g^{-1} 0.998
Intra-particle diffusion model	k_{id} C q_e R^2	3.261 mg $g^{-1}.min^{-0.5}$ 0.0054 6.53 mg g^{-1} 0.997

TABLE 4 The obtained Langmuir and Freundlich coefficients.

Isotherm model	Coefficient and variables
Langmuir isotherm model	k_l = 0.304 L mg^{-1} q_{max} = 8.16 mg g^{-1} R_L = 0.18 R^2 = 0.908
Freundlich isotherm model	k_f = 2.105 mg g^{-1} $\frac{1}{n}$ = 0.494 R^2 = 0.653

The data gathered from experiments were fitted with the plot and the value of k_{id} was estimated from the slope.

The mentioned kinetic models' data fitting is presented in Table 3.

A comparative analysis of the correlation coefficients (R^2 values) presented in Table 3 reveals significant differences in the performance of the kinetic models applied to the biosorption of Maxilon Red onto *Chlorella vulgaris* biomass. The pseudo-second-order kinetic model, characterized by a relatively low R^2 value of 0.877, demonstrates a poor fit and can therefore be reasonably excluded from further consideration. In contrast, the Elovich model shows a notably high R^2 value, suggesting a strong correlation with the experimental data. This implies that the adsorption process likely occurs on a heterogeneous surface, where the adsorption rate decreases over time due to the progressive occupation of active sites. As biosorption progresses, variations in surface heterogeneity or adsorption energy may arise, potentially caused by non-uniform site utilization or changes in the physicochemical properties of the microalgal surface. The intra-particle diffusion model also demonstrates a high R^2 value, underscoring the potential role of pore diffusion in the overall adsorption mechanism. This observation indicates that intra-particle transport significantly influences the migration of dye molecules within the biomass matrix. Furthermore, the pseudo-first-order model yields an R^2 value of 0.996, indicating a strong fit and suggesting that the adsorption rate is primarily controlled by the difference between

the equilibrium capacity and the amount adsorbed at a given time. This supports a rate-limiting step consistent with a linear adsorption mechanism. In addition to the high correlation, the pseudo-first-order model predicts an equilibrium biosorption capacity (q_e = 5.11 mg g^{-1}) nearly identical to the experimentally observed value ($q_{e,exp}$ = 5.12 mg g^{-1}). Although the Elovich model offers a marginally higher R^2 value (0.998), the 0.002 difference is negligible in practical terms. Moreover, the Elovich model underestimates the equilibrium capacity more substantially (q_e = 4.51 mg g^{-1}). Although the Elovich model had the best R^2, the authors favour the pseudo-first-order model based solely on the closeness of predicted and experimental q_e. Considering both the statistical goodness of fit and the superior agreement between the predicted and experimental q_e values, the pseudo-first-order model is identified as the most appropriate and reliable kinetic model for describing the biosorption behavior of Maxilon Red onto *C. vulgaris* biomass under the conditions studied.

Identifying the pseudo-first-order model as the most appropriate kinetic model for the biosorption of Maxilon Red onto *C. vulgaris* biomass holds significant scientific and practical value. The model's strong agreement with experimental data, reflected in a high correlation coefficient (R^2 = 0.996) and a predicted equilibrium adsorption capacity (q_e = 5.11 mg g^{-1}) that closely matches the experimental value (5.12 mg g^{-1}), enables accurate prediction of adsorption behavior and informs the design and optimization of treatment systems. This allows for precisely determining contact times, reactor sizing, and operational efficiency in dye removal processes. Moreover, the mechanical importance of a rate-limiting step driven by the difference between available adsorption sites and the amount adsorbed provides insight into surface-based sorption dynamics, suggesting potential improvements to biosorbent materials. The model also supports reliable scale-up from laboratory to industrial applications, reduces dependence on extensive experimentation, and enhances the credibility of economic and environmental examinations. Therefore, adopting the pseudo-first-order model offers theoretical understanding and enables the practical implementation of efficient, scalable, and sustainable biosorption systems.

3.3 Adsorption isotherm

The biosorption process by *C. vulgaris* was estimated using different Maxilon red concentrations using the Langmuir and Freundlich isotherm models. The red dye initial concentration (C_0) of 5, 10, 15, 20, 25, and 30 mg. L^{-1} reached the Ce of 1.32, 2.1, 2.2, 5.4, 9.5 and 14.1 mg. L^{-1}, respectively.

The Langmuir adsorption isotherm describes the monolayer biosorption of various metals onto bio sorbents. The Langmuir model is the most commonly used model for characterizing heterogeneous metal biosorption. The Langmuir adsorption isotherm is given in the following equation (Equation 8) (Pradhan et al., 2019).

$$\frac{C_e}{q_e} = \frac{1}{k_l q_{max}} + \frac{C_e}{q_{max}} \tag{8}$$

where, k_l represents the Langmuir binding constant (L. mg^{-1}), q_{max} is the maximum amount of Cr(III) adsorbed per unit weight of adsorbent (mg. g^{-1}). Consequently, a linear graph of $\frac{C_e}{q_e}$ vs C_e using experimental data illustrates the Langmuir isotherm parameters (slope = $\frac{1}{q_{max}}$, and intercept = $\frac{1}{k_l q_{max}}$). The Langmuir isotherm was then analyzed through the interpretation of the Langmuir equilibrium parameter (R_L), as given in Equation 9 (Maleki et al., 2015).

$$R_L = \frac{1}{1 + k_l C_0} \tag{9}$$

The value of R_L defines the nature of the biosorption process, it can be classified as below: unfavorable ($R_L > 1$), linear ($R_L = 1$), favorable ($0 < R_L < 1$), or irreversible ($R_L = 0$) (Sathvika et al., 2016).

The Freundlich model is understood to assume multilayer adsorption on heterogeneous surfaces. The model assumes that the adsorption sites are occupied in multilayers by the binding capacities. The model is expressed by the following Equation 10 (Pradhan et al., 2019).

$$\log(q_e) = \log k_f + 1/n \log C_e \tag{10}$$

where, k_f is the constant of Freundlich isotherm ($mg.g^{-1}$) which is related to adsorption capacity, and $1/n$ is another constant related to the intensity of biosorption. $1/n$ is a value that characterizes the practicability of the isotherm, e.g., irreversible ($1/n = 0$); favorable ($0 < 1/n < 1$); unfavorable ($1/n > 1$). By plotting $\log(q_e)$ against $\log(C_e)$ using experimental data, $1/n$ and $\log k_f$ will be realized as the line slope and intercept, respectively. Furthermore, the calculated parameters of the Langmuir and the Freundlich isotherm models are shown in Table 4.

The poor value of R^2 of the Freundlich model (0.653) in comparison with the R^2 value for the Langmuir model (0.908) shows that the Langmuir model generated a more accurate fit to the experimental data. Meaning that adsorption occurs in a single layer on a homogeneous surface with a finite number of specific adsorption sites. Once the aforementioned sites are filled, no further adsorption can happen, which suggests that the adsorbent has a maximum capacity, represented as q_{max}. The model is predicated on the assumption that there is no interaction between adsorbed molecules and that all adsorption sites have the same capacity for the adsorbate. This makes it suitable for uniform surface adsorption processes (Pradhan et al., 2019). The resulting values for R_L were 0.18 for the C_0 of 15 mg. L^{-1}. The results of the calculations suggest that the Maxilon red dye biosorption process onto the microalgae biomass was a favorable one.

3.4 Dye removal performance with continuous dynamic membrane photobioreactor

The optimal concentration for maximum dye removal in the PBR system as batch mode of operation was determined to be 15 mg. L^{-1}. This approach uses the same ideal dye loading conditions to evaluate the performance of batch PBR and continuous DMPBR. Figure 4 represents the removal efficiency of Maxilon Red when DMPBR is used, which is the continuous mode. The removal efficiency of dye removal is almost constant during the 10 h of operation and almost full dye removal can be reached 98% for initial

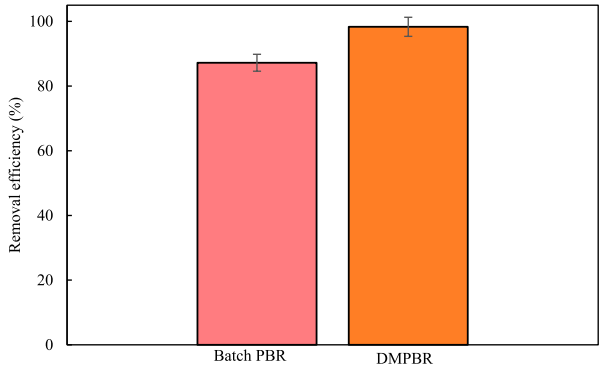

FIGURE 4
Maxilon red dye removal efficiency *versus* time (dye initial concentration 15 mg. L^{-1}) via batch PBR and continuous DMPBR. (The experiment was conducted in triplicate (n = 3)).

dye concentrations of 15 mg. L^{-1} Utilizing a DM offers a distinct advantage, as it ensures the maintenance of physical separation even after achieving equilibrium in the batch PBR after 2.5 h. This characteristic enhances the overall efficiency of the biosorption system, surpassing the efficiency of a single biosorption system. This suggests a potential for synergistic use of suspended biosorbent and microalgal DM in a DMPBR. These findings suggest that the DMPBR system's synergy with suspended biosorbents and a dynamic membrane optimizes overall performance despite fouling's limitations. Statistical analysis showed a significant effect on the dye removal efficiency by incorporating a DM into the system (p-value$<$0.05).

When comparing these results with the ones from the literature (Berkessa et al., 2020), they had reached almost 98% of Remazol Brilliant Blue R (~50% pure) removal in a reactor with working volume of 10 L. The dynamic membrane, with total filtration area of 0.01 m^2, was immersed in the cylindrical side stream reactor with a volume of 4 L (Berkessa et al., 2020).

Although the present results show that DMPBR cannot remove the dye much more than anaerobic dynamic membrane reactor and living membrane bioreactor (almost 98% for all cases). However, it can be argued that the potential of the current research is its green nature, meaning that it is less harmful to the environment and produces no dangerous chemicals.

3.5 FTIR analysis

The spectral analysis was conducted within the range of 400 to 4,000 cm^{-1}. It was determined that the cell walls of microalgae contain a variety of chemical groups, including hydroxyl, carbonyl, and sulfhydryl, and it is the responsibility of these proteins to determine the adsorption ability of the microalgal cell (Pradhan et al., 2019). As illustrated in Figure 5, the FTIR spectra demonstrates *Chlorella vulgaris* microalgae before and after Maxilon Red dye adsorption.

The broad O-H stretching band at 3425 cm^{-1} shifts to 3480 cm^{-1} with reduced intensity after dye adsorption, indicating the interaction of hydroxyl groups with the dye molecules, likely through hydrogen bonding (Chin et al., 2020). A shift of the C=O stretching peak from 1635 cm^{-1} to 1665 cm^{-1} suggests that carbonyl groups, possibly from ketones, aldehydes, carboxylic acids, primary amides, and esters, which are involved in the dye binding (Peng et al., 2015). The peak at 2100 cm^{-1} wavenumber generally corresponds to the stretching of a carbon-carbon triple bond (C≡C), typical of alkyne groups, although it can also be associated with nitrile groups (C≡N) in some cases. Upon adsorption of Maxilon red dye, this peak disappeared, suggesting a significant interaction between the dye and the functional groups responsible for this absorption. The 710 cm^{-1} peak is the most significant in the fingerprint region and correlates with aliphatic chloro compounds, C-Cl stretch, and has disappeared due to dye adsorption. This phenomenon can result in a modification of the vibrational frequencies of the functional groups present on the surface of the biomass. The binding of sorbate to functional groups, such as carboxyl (-COO-), hydroxyl (-OH), amino ($-NH_4$), or phosphate ($-PO_4^{-3}$), has the potential to alter the associated peaks in the fingerprint region resulting in a decrease in wave number (Tattibayeva et al., 2022). The peak at 1040 cm^{-1}, associated with C-O stretching vibrations in polysaccharides or C-N stretching in proteins (Croué et al., 2003), showed a potential increase in intensity after dye adsorption. This could be due to the surface adsorption of dye molecules, hydrogen bonding interactions, or the formation of weak new C-O bonds resulting from the interaction of dye molecules with the polysaccharides and proteins in the microalgae cell wall (Pradhan et al., 2019). These results underscore the complexity of the adsorption process and reinforce the potential of *Chlorella vulgaris* as a promising biosorbent for dye removal.

3.6 SEM analysis

Figures 6a,b shows SEM images of *C. vulgaris* before dye removal, and with adsorbed dye on the microalgal dynamic membrane, respectively, with magnification of 1000X.

SEM micrographs (Figure 5) display the morphological changes. Raw *Chlorella vulgaris* cells have smooth, spherical surfaces before dye adsorption (Figure 5a). On the contrary, the microalgal DM after dye adsorption shows a heterogeneous, porous, biofilm-like layer packed with irregular aggregates after dye treatment (Figure 5b). This texture and multilayered structure result from the deposition of microalgal cells, extracellular polymeric substances (EPS), and adsorbed dye particles. The participation of the hydroxyl and carbonyl groups in the FTIR shows that the EPS matrix forms the cake layer that forms the DM's physical barrier in addition to capturing dye molecules (Liao et al., 2018). By overcoming equilibrium constraints and continuously renewing binding sites within the EPS matrix while maintaining a structured cake layer, the DMPBR enhances contact between biomass and dye, which explains why it outperforms the batch PBR (Diaz-Uribe et al., 2021).

3.7 DMPBR and circular economy

DMPBR offers a promising method for a circular economy by considering wastewater not as a pollutant but as a resource (Goh

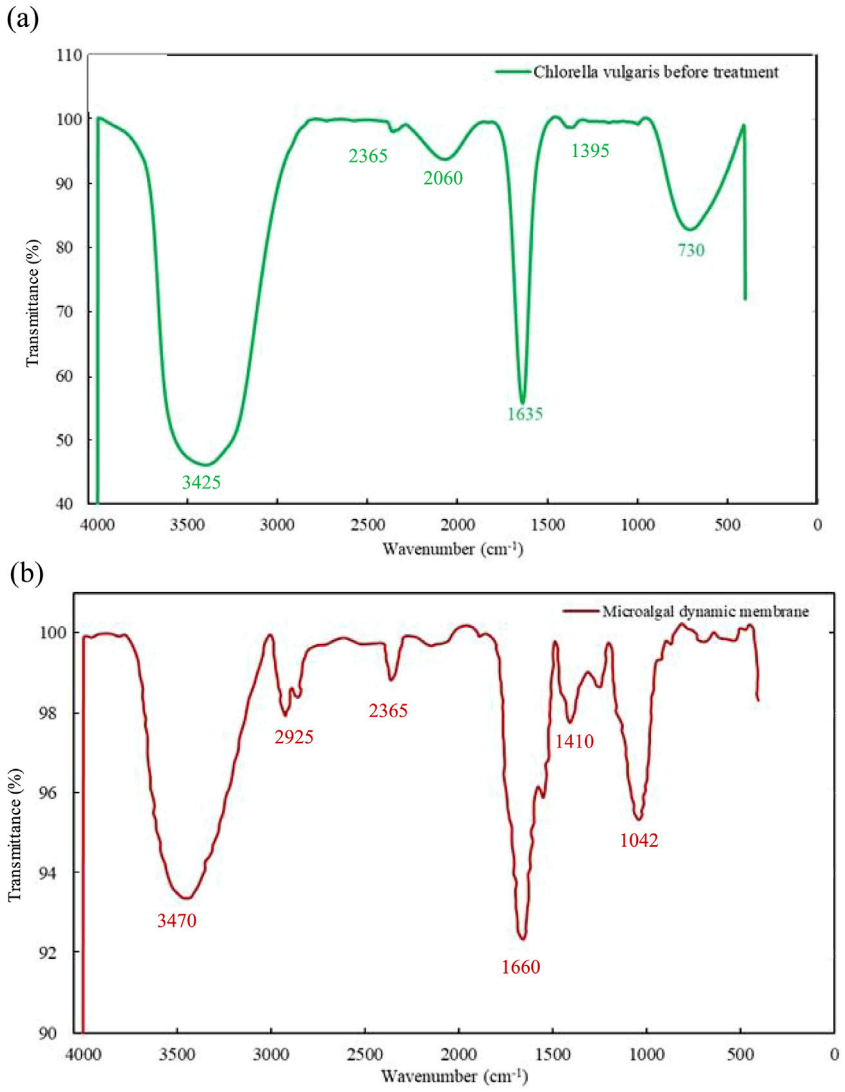

FIGURE 5
FTIR analysis of red dye adsorption using *Chlorella vulgaris* microalgae; **(a)** Pure *Chlorella vulgaris* suspension; **(b)** Dynamic membrane after dye treatment.

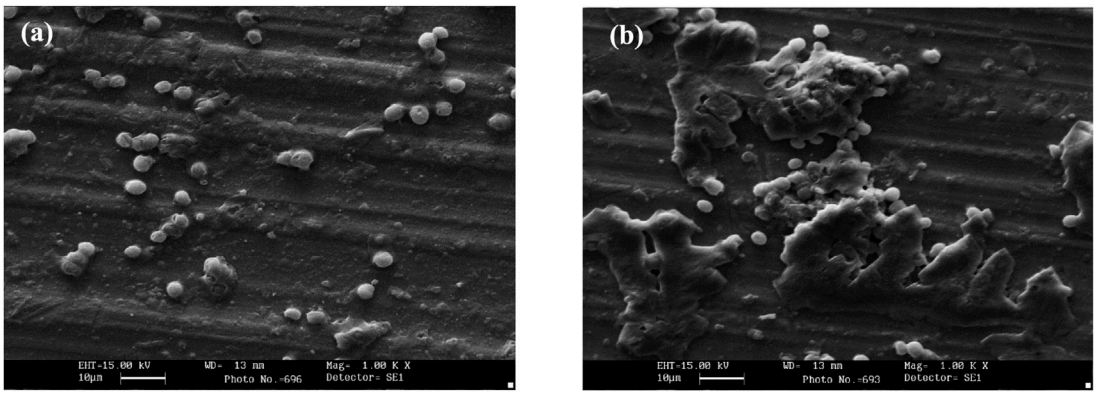

FIGURE 6
SEM images of **(a)** raw *Chlorella vulgaris* suspension; **(b)** adsorbed dye on microalgal dynamic membranes.

et al., 2022). Textile wastewater contains effluents such as nitrate and phosphate, which would benefit microalgae growth, enabling simultaneous wastewater treatment, Maxilon red dye removal, and biomass generation. The dynamic membrane formed on the membrane's surface improves wastewater removal and offers a low-energy alternative to conventional PBR systems (Liao et al., 2024). This study shows that DMPBRs are highly effective for Maxilon red dye removal. Moreover, the photosynthetic-based nature of microalgae would allow the occurrence of CO_2 capturing at the same time as microalgae cells require CO_2 for growth (Liao et al., 2024).

Furthermore, by optimizing resource use and reducing waste, the biomass produced in the DMPBR may be sustainably recycled into high-value products, supporting the zero-waste biorefinery concept. One important use is creating thin-film composite (TFC) membranes, which provide an economical and sustainable substitute for conventional materials. These membranes, which are made from algae biomass cultivated in wastewater, exhibit durability and robustness for a range of industrial applications, including organic solvent nanofiltration (OSN) systems, thus promoting the ideas of green chemistry. Furthermore, the biomass can be utilized to create carbonaceous anodes for lithium-ion batteries and optically pure (R)-γ-valerolactone ((R)-GVL) for biopharmaceuticals and bioplastics, which will help create more sophisticated energy storage systems and lower CO_2 emissions (Yang et al., 2023; Cha et al., 2024).

However, the feasibility of dye recovery remains a challenge. The reason is that most dyes (such as Maxilon red) undergo structural transformation or degradation during the treatment period, making them unusable for reuse; nevertheless, although partial recovery is theoretically possible, whether this recovered dye is efficient or economically logical needs further research and discussion (Sarioglu and Aşkal, 2018; Pimentel et al., 2023). Therefore, it is recommended that DMPBRs be used for resource recovery, pollutant neutralization, and wastewater treatment rather than dye recovery (Goh et al., 2022; Liao et al., 2024).

4 Conclusion

The discharge of dye-contaminated wastewater from textile and dye-processing industries presents a persistent environmental challenge. This study compared a conventional batch photobioreactor (PBR) to a dynamic membrane photobioreactor (DMPBR) operating in continuous mode, both employing *C. vulgaris* for the removal of Maxilon Red dye. The batch PBR achieved high initial removal rates but was limited by biosorption equilibrium, beyond which no further dye removal occurred. In contrast, the continuous DMPBR maintained a consistently high removal efficiency (~98%), effectively overcoming biosorption saturation and enhancing system stability, effluent quality, and biomass productivity. While these results demonstrate the promise of DMPBRs as efficient and eco-friendly systems for textile wastewater treatment, several limitations must be mentioned. First, the system's performance was analyzed under controlled laboratory conditions using synthetic wastewater; hence, scalability and robustness under real, complex textile effluents remain to be fully validated. Second, although dynamic membranes improve filtration, long-term operation may still lead to performance decline due to biofouling or EPS accumulation, which requires further monitoring and optimization. Third, dye recovery remains technically challenging, as most dyes undergo partial degradation or irreversible binding, reducing their reuse potential. Finally, while microalgal biomass offers opportunities for valorization, its safety and market viability depend on stringent downstream processing to ensure removal of residual pollutants. Future work should focus on pilot-scale validation with real wastewater, techno-economic analysis, and development of integrated valorization pathways to fully realize the circular economy potential of microalgal DMPBR systems.

Data availability statement

The original contributions presented in the study are included in the article/supplementary material, further inquiries can be directed to the corresponding author.

Author contributions

SF: Writing – review and editing, Writing – original draft, Investigation, Formal analysis. IA: Writing – original draft, Investigation, Formal analysis, Writing – review and editing. ME: Investigation, Writing – original draft, Formal analysis, Conceptualization, Validation, Writing – review and editing. SH: Conceptualization, Writing – original draft, Validation, Investigation, Formal analysis, Writing – review and editing. GL: Writing – original draft. MH: Writing – review and editing, Writing – original draft, Supervision. FP: Writing – original draft, Project administration, Conceptualization, Writing – review and editing.

Funding

The author(s) declare that no financial support was received for the research and/or publication of this article.

Conflict of interest

The authors declare that the research was conducted in the absence of any commercial or financial relationships that could be construed as a potential conflict of interest.

Generative AI statement

The author(s) declare that no Generative AI was used in the creation of this manuscript.

Publisher's note

References

Acuner, E., and Dilek, F. B. (2004). Treatment of tectilon yellow 2G by Chlorella vulgaris. *Process Biochem.* 39, 623–631. doi:10.1016/s0032-9592(03)00138-9

Al-Amrani, W. A., Hanafiah, M. A. K. M., and Mohammed, A.-H. A. (2022). A comprehensive review of anionic azo dyes adsorption on surface-functionalised silicas. *Environ. Sci. Pollut. Res.* 29, 76565–76610. doi:10.1007/s11356-022-23062-0

Al-Tohamy, R., Ali, S. S., Li, F., Okasha, K. M., Mahmoud, Y.A.-G., Elsamahy, T., et al. (2022). A critical review on the treatment of dye-containing wastewater: ecotoxicological and health concerns of textile dyes and possible remediation approaches for environmental safety. *Ecotoxicol. Environ. Saf.* 231, 113160. doi:10.1016/j.ecoenv.2021.113160

Álvarez-González, A., Uggetti, E., Serrano, L., Gorchs, G., Casas, M. E., Matamoros, V., et al. (2023). The potential of wastewater grown microalgae for agricultural purposes: contaminants of emerging concern, heavy metals and pathogens assessment. *Environ. Pollut.* 324, 121399. doi:10.1016/j.envpol.2023.121399

Bahadur, N., Das, P., and Bhargava, N. (2020). Improving energy efficiency and economic feasibility of photocatalytic treatment of synthetic and real textile wastewater using bagasse fly ash modified TiO2. *Chem. Eng. J. Adv.* 2, 100012. doi:10.1016/j.ceja.2020.100012

Barani, M., Helchi, S., Shirazi, M. M. A., Emamshoushtari, M. M., Pajoum Shariati, F., and Bazgir, S. (2025). Investigation of biomass and pollutant kinetics in batch bioreactors for effective industrial oily wastewater treatment. *J. Water Process Eng.* 70, 107115. doi:10.1016/j.jwpe.2025.107115

Berkessa, Y. W., Yan, B., Li, T., Jegatheesan, V., and Zhang, Y. (2020). Treatment of anthraquinone dye textile wastewater using anaerobic dynamic membrane bioreactor: performance and microbial dynamics. *Chemosphere* 238, 124539. doi:10.1016/j.chemosphere.2019.124539

Cha, J., Lim, C.-H., Lee, J., Lim, J.-K., Kim, M., Park, W.-K., et al. (2024). Algal biomass-based zero-waste biorefinery for producing optically pure (R)-γ-valerolactone and carbonaceous electrodes applicable for energy storage devices. *Chem. Eng. J.* 490, 151713. doi:10.1016/j.cej.2024.151713

Chan, A., Salsali, H., and McBean, E. (2014). Heavy metal removal (copper and zinc) in secondary effluent from wastewater treatment plants by microalgae. *ACS Sustain. Chem. Eng.* 2, 130–137. doi:10.1021/sc400289z

Chin, J. Y., Chng, L. M., Leong, S. S., Yeap, S. P., Yasin, N. H. M., and Toh, P. Y. (2020). Removal of synthetic dye by Chlorella vulgaris microalgae as natural adsorbent. *Arab. J. Sci. Eng.* 45, 7385–7395. doi:10.1007/s13369-020-04557-9

Chung, K.-T. (2016). Azo dyes and human health: a review. *J. Environ. Sci. Heal. Part C* 34, 233–261. doi:10.1080/10590501.2016.1236602

Corona-Bautista, M., Picos-Benítez, A., Villaseñor-Basulto, D., Bandala, E., and Peralta-Hernández, J. M. (2021). Discoloration of azo dye brown HT using different advanced oxidation processes. *Chemosphere* 267, 129234. doi:10.1016/j.chemosphere.2020.129234

Croué, J.-P., Benedetti, M. F., Violleau, D., and Leenheer, J. A. (2003). Characterization and copper binding of humic and nonhumic organic matter isolated from the South Platte River: evidence for the presence of nitrogenous binding site. *Environ. Sci. Technol.* 37, 328–336. doi:10.1021/es020676p

da Rosa, A. L. D., Carissimi, E., Dotto, G. L., Sander, H., and Feris, L. A. (2018). Biosorption of rhodamine B dye from dyeing stones effluents using the green microalgae Chlorella pyrenoidosa. *J. Clean. Prod.* 198, 1302–1310. doi:10.1016/j.jclepro.2018.07.128

Deniz, F. (2014). Effective removal of Maxilon Red GRL from aqueous solutions by walnut shell: nonlinear kinetic and equilibrium models. *Environ. Prog. Sustain. Energy* 33, 396–401. doi:10.1002/ep.11797

Desore, A., and Narula, S. A. (2018). An overview on corporate response towards sustainability issues in textile industry. *Environ. Dev. Sustain.* 20, 1439–1459. doi:10.1007/s10668-017-9949-1

Diaz-Uribe, C., Angulo, B., Patiño, K., Hernández, V., Vallejo, W., Gallego-Cartagena, E., et al. (2021). Cyanobacterial biomass as a potential biosorbent for the removal of recalcitrant dyes from water. *Water* 13, 3176. doi:10.3390/w13223176

El Gaayda, J., Titchou, F.-E., Karmal, I., Barra, I., Errami, M., Yap, P.-S., et al. (2024). Application of grape seed and Austrocylindropuntia mucilage for the simultaneous removal of azo dye and turbidity from synthetic wastewater: optimizing experimental conditions using Box-Behnken Design (BBD). *J. Water Process Eng.* 58, 104718. doi:10.1016/j.jwpe.2023.104718

Emamshoushtari, M. M., Helchi, S., Pajoum Shariati, F., Lotfi, M., and Hemmati, A. (2022). An investigation into the efficiency of microalgal dynamic membrane photobioreactor in nickel removal from synthesized vegetable oil industry wastewater: a water energy nexus case study. *Energy Nexus* 7, 100116. doi:10.1016/j.nexus.2022.100116

Ezhumalai, G., and Rajkumar, R. (2025). Enhanced biomass and lipid production of Chlorella vulgaris through the utilization of municipal wastewater as a nutrient source: a sustainable feedstock for biodiesel production. *Biomass Convers. Biorefinery* 15, 14853–14868. doi:10.1007/s13399-024-06380-w

Fard, G. H., and Mehrnia, M. R. (2017). Investigation of mercury removal by Micro-Algae dynamic membrane bioreactor from simulated dental waste water. *J. Environ. Chem. Eng.* 5, 366–372. doi:10.1016/j.jece.2016.11.031

Farouq, R. (2022). Coupling adsorption-photocatalytic degradation of methylene blue and maxilon red. *J. Fluoresc.* 32, 1381–1388. doi:10.1007/s10895-022-02934-1

Faruque, M. O., Uddin, S., Hossain, M. M., Hossain, S. M. Z., Shafiquzzaman, M., and Razzak, S. A. (2024). A comprehensive review on microalgae-driven heavy metals removal from industrial wastewater using living and nonliving microalgae. *J. Hazard. Mater. Adv.* 16, 100492. doi:10.1016/j.hazadv.2024.100492

Fazal, T., Rehman, M. S. U., Javed, F., Akhtar, M., Mushtaq, A., Hafeez, A., et al. (2021). Integrating bioremediation of textile wastewater with biodiesel production using microalgae (Chlorella vulgaris). *Chemosphere* 281, 130758. doi:10.1016/j.chemosphere.2021.130758

Goh, P. S., Ahmad, N. A., Lim, J. W., Liang, Y. Y., Kang, H. S., Ismail, A. F., et al. (2022). Microalgae-enabled wastewater remediation and nutrient recovery through membrane photobioreactors: recent achievements and future perspective. *Membr. (Basel)* 12, 1094. doi:10.3390/membranes12111094

Gupta, V.K., and Suhas. (2009). Application of low-cost adsorbents for dye removal–a review. *J. Environ. Manage.* 90, 2313–2342. doi:10.1016/j.jenvman.2008.11.017

Gupta, P. L., Lee, S.-M., and Choi, H.-J. (2015). A mini review: photobioreactors for large scale algal cultivation. *World J. Microbiol. Biotechnol.* 31, 1409–1417. doi:10.1007/s11274-015-1892-4

Hamous, H., Khenifi, A., Orts, F., Bonastre, J., and Cases, F. (2021). Carbon textiles electrodes modified with RGO and Pt nanoparticles used for electrochemical treatment of azo dye. *J. Electroanal. Chem.* 887, 115154. doi:10.1016/j.jelechem.2021.115154

Helchi, S., Pajoum Shariati, F., Emamshoushtari, M. M., Sohani, E., Moayed Mohseni, M., and Bonakdarpour, B. (2023). The hydrodynamic characterization of an oval airlift open pond (AOP) in the air–water system. *Chem. Eng. Commun.* 210, 1853–1863. doi:10.1080/00986445.2022.2150616

Hernández-Zamora, M., Cristiani-Urbina, E., Martínez-Jerónimo, F., Perales-Vela, H. V., Ponce-Noyola, T., Montes-Horcasitas, M. del C., et al. (2015). Bioremoval of the azo dye Congo Red by the microalga Chlorella vulgaris. *Environ. Sci. Pollut. Res.* 22, 10811–10823. doi:10.1007/s11356-015-4277-1

Jallouli, S., Buonerba, A., Borea, L., Hasan, S. W., Belgiorno, V., Ksibi, M., et al. (2023). Living membrane bioreactor for highly effective and eco-friendly treatment of textile wastewater. *Sci. Total Environ.* 871, 161963. doi:10.1016/j.scitotenv.2023.161963

Jankowska, K., Su, Z., Zdarta, J., Jesionowski, T., and Pinelo, M. (2022). Synergistic action of laccase treatment and membrane filtration during removal of azo dyes in an enzymatic membrane reactor upgraded with electrospun fibers. *J. Hazard. Mater.* 435, 129071. doi:10.1016/j.jhazmat.2022.129071

Jegatheesan, V., Pramanik, B. K., Chen, J., Navaratna, D., Chang, C.-Y., and Shu, L. (2016). Treatment of textile wastewater with membrane bioreactor: a critical review. *Bioresour. Technol.* 204, 202–212. doi:10.1016/j.biortech.2016.01.006

Kanwal, S., Mehran, M. T., Hassan, M., Anwar, M., Naqvi, S. R., and Khoja, A. H. (2022). An integrated future approach for the energy security of Pakistan: replacement of fossil fuels with syngas for better environment and socio-economic development. *Renew. Sustain. Energy Rev.* 156, 111978. doi:10.1016/j.rser.2021.111978

Keyvan Hosseini, M., Keyvan Hosseini, P., Helchi, S., and Pajoum Shariati, F. (2023). The comparison between two methods of membrane cleaning to control membrane fouling in a hybrid membrane photobioreactor (HMPBR). *Prep. Biochem. Biotechnol.* 53, 394–400. doi:10.1080/10826068.2022.2095574

Kishor, R., Purchase, D., Saratale, G. D., Ferreira, L. F. R., Bilal, M., Iqbal, H. M. N., et al. (2021). Environment friendly degradation and detoxification of Congo red dye and textile industry wastewater by a newly isolated Bacillus cohnni (RKS9). *Environ. Technol. Innov.* 22, 101425. doi:10.1016/j.eti.2021.101425

Liao, Y., Bokhary, A., Maleki, E., and Liao, B. (2018). A review of membrane fouling and its control in algal-related membrane processes. *Bioresour. Technol.* 264, 343–358. doi:10.1016/j.biortech.2018.06.102

Liao, Y., Fatehi, P., and Liao, B. (2024). A Study of theoretical analysis and modelling of microalgal membrane photobioreactors for microalgal biomass production and nutrient removal. *Membr. (Basel)* 14, 245. doi:10.3390/membranes14120245

Lim, S.-L., Chu, W.-L., and Phang, S.-M. (2010). Use of Chlorella vulgaris for bioremediation of textile wastewater. *Bioresour. Technol.* 101, 7314–7322. doi:10.1016/j.biortech.2010.04.092

López-Sánchez, A., Silva-Gálvez, A. L., Aguilar-Juárez, Ó., Senés-Guerrero, C., Orozco-Nunnelly, D. A., Carrillo-Nieves, D., et al. (2022). Microalgae-based livestock wastewater treatment (MbWT) as a circular bioeconomy approach: enhancement of biomass productivity, pollutant removal and high-value compound production. *J. Environ. Manage.* 308, 114612. doi:10.1016/j.jenvman.2022.114612

Madadi, R., Zahed, M. A., Pourbabaee, A. A., Tabatabaei, M., and Naghavi, M. R. (2021). Simultaneous phycoremediation of petrochemical wastewater and lipid production by Chlorella vulgaris. *SN Appl. Sci.* 3, 505–510. doi:10.1007/s42452-021-04511-w

Maleki, A., Hayati, B., Naghizadeh, M., and Joo, S. W. (2015). Adsorption of hexavalent chromium by metal organic frameworks from aqueous solution. *J. Ind. Eng. Chem.* 28, 211–216. doi:10.1016/j.jiec.2015.02.016

Moradi, Z., Haghjou, M. M., Zarei, M., and Sharifan, H. (2024). Harnessing Chlorella vulgaris for the phycoremediation of azo dye: a comprehensive analysis of metabolic responses and antioxidant system. *Algal Res.* 82, 103660. doi:10.1016/j.algal.2024.103660

Nasser, T., Emamshoushtari, M. M., Helchi, S., Saeidi, A., and Pajoum Shariati, F. (2023). Mitigating membrane fouling in an internal loop airlift membrane photobioreactor containing Spirulina platensis: effects of riser cross-sectional area and hydrophilic baffles. *Prep. Biochem. Biotechnol.* 54, 779–787. doi:10.1080/10826068.2023.2283765

Özcan, A. S., Erdem, B., and Özcan, A. (2005). Adsorption of Acid Blue 193 from aqueous solutions onto BTMA-bentonite. *Colloids Surfaces A Physicochem. Eng. Asp.* 266, 73–81. doi:10.1016/j.colsurfa.2005.06.001

Park, S., Lee, S.-J., Noh, W., Kim, Y. J., Kim, J.-H., Back, S.-M., et al. (2024). Production of safe cyanobacterial biomass for animal feed using wastewater and drinking water treatment residuals. *Heliyon* 10, e25136. doi:10.1016/j.heliyon.2024.e25136

Peng, X., Ma, X., Lin, Y., Guo, Z., Hu, S., Ning, X., et al. (2015). Co-pyrolysis between microalgae and textile dyeing sludge by TG–FTIR: kinetics and products. *Energy Convers. Manag.* 100, 391–402. doi:10.1016/j.enconman.2015.05.025

Pimentel, C. H., Freire, M. S., Gómez-Díaz, D., and González-Álvarez, J. (2023). Removal of wood dyes from aqueous solutions by sorption on untreated pine (Pinus radiata) sawdust. *Cellulose* 30, 4587–4608. doi:10.1007/s10570-023-05145-4

Pradhan, D., Sukla, L. B., Mishra, B. B., and Devi, N. (2019). Biosorption for removal of hexavalent chromium using microalgae Scenedesmus sp. *J. Clean. Prod.* 209, 617–629. doi:10.1016/j.jclepro.2018.10.288

Rafatullah, M., Ismail, S., and Ahmad, A. (2019). Optimization study for the desorption of methylene blue dye from clay based adsorbent coating. *Water* 11, 1304. doi:10.3390/w11061304

Rehman, R., Iqbal, J., Ur Rehman, M. S., Hamid, S., Wang, Y., Rasool, K., et al. (2024). Algal-biochar and Chlorella vulgaris microalgae: a sustainable approach for textile wastewater treatment and biodiesel production. *Biochar* 6, 65. doi:10.1007/s42773-024-00358-7

Rüdisüli, M., Schildhauer, T. J., Biollaz, S. M. A., and Van Ommen, J. R. (2012). Scale-up of bubbling fluidized bed reactors—A review. *Powder Technol.* 217, 21–38. doi:10.1016/j.powtec.2011.10.004

Saadaoui, I., Rasheed, R., Aguilar, A., Cherif, M., Al Jabri, H., Sayadi, S., et al. (2021). Microalgal-based feed: promising alternative feedstocks for livestock and poultry production. *J. Anim. Sci. Biotechnol.* 12, 76. doi:10.1186/s40104-021-00593-z

Sarioglu, M., and Aşkal, M. (2018). Biosorption of azo dye (Maxilon Red and Everzol Red) on to natural and modified waste sludge. *Global NEST J.* 20 (1), 25–32.

Sarma, U., Hoque, M. E., Thekkangil, A., Venkatarayappa, N., and Rajagopal, S. (2024). Microalgae in removing heavy metals from wastewater–An advanced green technology for urban wastewater treatment. *J. Hazard. Mater. Adv.* 15, 100444. doi:10.1016/j.hazadv.2024.100444

Sathvika, Manasi, T., Rajesh, V., and Rajesh, N. (2016). Adsorption of chromium supported with various column modelling studies through the synergistic influence of Aspergillus and cellulose. *J. Environ. Chem. Eng.* 4, 3193–3204. doi:10.1016/j.jece.2016.06.027

Shirazi, Y., Helchi, S., Emamshoushtari, M. M., Niakan, S., Sohani, E., and Pajoum Shariati, F. (2024). The effect of different light spectra on selenium bioaccumulation by Spirulina platensis Cyanobacteria in flat plate photobioreactors. *Prep. Biochem. Biotechnol.* 55, 491–501. doi:10.1080/10826068.2024.2426744

Siddique, K., Rizwan, M., Shahid, M. J., Ali, S., Ahmad, R., and Rizvi, H. (2017). in *Textile wastewater treatment options: a critical review BT - enhancing cleanup of environmental pollutants: volume 2: Non-Biological approaches*. Editors N. A. Anjum, S. S. Gill, and N. Tuteja (Cham: Springer International Publishing), 183–207.

Sreedharan, V., and Bhaskara Rao, K. V. (2019). in *Biodegradation of textile Azo dyes BT - Nanoscience and biotechnology for environmental applications*. Editors K. M. Gothandam, S. Ranjan, N. Dasgupta, and E. Lichtfouse (Cham: Springer International Publishing), 115–139.

Swain, S. K., Sahoo, A., Majhi, S. K., Phaomei, G., Sahoo, N. K., and Tripathy, S. K. (2023). Unveiling the synergistic effect of magnetite and ZrPO4 for highly selective removal of Anionic Azo dyes *via* an ion-exchange process. *ACS Appl. Eng. Mater.* 1, 3016–3026. doi:10.1021/acsaenm.3c00492

Tattibayeva, Z., Tazhibayeva, S., Kujawski, W., Zayadan, B., and Musabekov, K. (2022). *Peculiarities of adsorption of Cr (VI) ions on the surface of Chlorella vulgaris ZBS1 algae cells*. *Heliyon* 8, e10468. doi:10.1016/j.heliyon.2022.e10468

Vaezi, M., Helchi, S., Pajoum Shariati, F., Emamshoushtari, M. M., Keyvan Hosseini, M., Keyvan Hosseini, P., et al. (2025). Performance of a novel hybrid membrane bioreactor (HMBR) treating synthetic dairy wastewater: assessment of coupled mechanical removal sections and MBR. *Clean. Technol. Environ. Policy* 17, 17–28. doi:10.1007/s10098-024-02801-6

Wang, J., Song, A., Huang, Y., Liao, Q., Xia, A., Zhu, X., et al. (2021). Domesticating Chlorella vulgaris with gradually increased the concentration of digested piggery wastewater to bio-remove ammonia nitrogen. *Algal Res.* 60, 102526. doi:10.1016/j.algal.2021.102526

Yadav, M., Rani, K., Sandal, N., and Chauhan, M. K. (2022). An approach towards safe and sustainable use of the green alga Chlorella for removal of radionuclides and heavy metal ions. *J. Appl. Phycol.* 34, 2117–2133. doi:10.1007/s10811-022-02771-6

Yagub, M. T., Sen, T. K., and Ang, H. M. (2012). Equilibrium, kinetics, and thermodynamics of methylene blue adsorption by pine tree leaves. *Soil Pollut.* 223, 5267–5282. doi:10.1007/s11270-012-1277-3

Yagub, M. T., Sen, T. K., Afroze, S., and Ang, H. M. (2014). Dye and its removal from aqueous solution by adsorption: a review. *Adv. Colloid Interface Sci.* 209, 172–184. doi:10.1016/j.cis.2014.04.002

Yang, C., Cavalcante, J., de Freitas, B. B., Lauersen, K. J., and Szekely, G. (2023). Crude algal biomass for the generation of thin-film composite solvent-resistant nanofiltration membranes. *Chem. Eng. J.* 470, 144153. doi:10.1016/j.cej.2023.144153

Yaseen, D. A., and Scholz, M. (2019). Textile dye wastewater characteristics and constituents of synthetic effluents: a critical review. *Int. J. Environ. Sci. Technol.* 16, 1193–1226. doi:10.1007/s13762-018-2130-z

Zhang, X., and Lu, Q. (2024). Cultivation of microalgae in food processing effluent for pollution attenuation and astaxanthin production: a review of technological innovation and downstream application. *Front. Bioeng. Biotechnol.* 12, 1365514. doi:10.3389/fbioe.2024.1365514

Zhang, J., Zhou, Q., and Ou, L. (2012). Kinetic, isotherm, and thermodynamic studies of the adsorption of Methyl Orange from aqueous solution by Chitosan/Alumina composite. *J. Chem. Eng. Data* 57, 412–419. doi:10.1021/je2009945

Zheng, T., Li, J., Ji, Y., Zhang, W., Fang, Y., Xin, F., et al. (2020). Progress and prospects of bioelectrochemical systems: electron transfer and its applications in the microbial metabolism. *Front. Bioeng. Biotechnol.* 8, 10. doi:10.3389/fbioe.2020.00010